Diffusion Changes in a Tumor and Peritumoral Tissue After Stereotactic Irradiation for Brain Tumors: Possible Prediction of Treatment Response

Noriaki Tomura, MD, Komei Narita, RT,‡ Jun-ichi Izumi, MD,* Akira Suzuki, MD,† Akira Anbai, MD,* Takahiro Otani, MD,* Ikuo Sakuma, MD,* Satoshi Takahashi, MD,* Kazuo Mizoi, MD,† and Jiro Watarai, MD**

Objective: Changes in apparent diffusion coefficient (ADC) in a tumor and peritumoral tissue after stereotactic irradiation (STI) were evaluated, and then the therapeutic efficacy of ADC measurement was assessed.
Methods: In 20 tumors, diffusion-weighted imaging within 1 week before and 2–4 weeks after STI was performed. The normalized ADC (nADC) was measured. The nADCs in the tumor and peritumoral region before STI were compared with those after STI and the change in tumor nADC compared with the change in tumor size.
Results: The nADC of the tumors was significantly higher 2–4 weeks after STI compared with that before STI. The nADC of the peritumoral regions 2–4 weeks after STI did not differ significantly from that before STI. A significant difference in the nADC at 2–4 weeks after STI was observed between the responder and nonresponder groups.
Conclusions: Changes in nADC as measured by diffusion-weighted imaging can predict response to STI.

Key Words: stereotactic irradiation, ADC, brain, neoplasm

(*J Comput Assist Tomogr* 2006;30:496–500)

Stereotactic irradiation (STI), including stereotactic radiosurgery and fractionated stereotactic radiotherapy, has been widely used to treat cerebral metastatic tumors[1] and other cerebral tumors such as gliomas,[2] meningiomas,[3] and schwannomas.[4] To determine the response of a tumor to STI using imaging, positron emission tomography using F-18-fluorodeoxyglucose (FDG-PET),[5–7] single photon emission computed tomography using thallium-201 (Tl-SPECT)[8–10] instead of conventional computed tomography (CT), and magnetic resonance imaging (MRI) have been used.

Diffusion-weighted MRI (DWI) is widely used to detect acute ischemic lesions, as a restriction in water diffusion occurs in affected brain tissue. DWI has also been used to evaluate tumor diffusivity, which is restricted in malignant tumors such as malignant lymphomas.[11–13] The apparent diffusion coefficient (ADC) is thought to depend on extracellular and intracellular components.[11,14] In malignant tumors, such as malignant lymphomas, a decreased ADC is observed due to a reduced extracellular component. The ADC may increase after radiation therapy, including STI, as a result of cell death and increased permeability; however, only few studies have examined the changes in ADC in human tumors after chemotherapy or radiotherapy.[15–18] In the present study, changes in the ADC of tumor and peritumoral tissue after STI were evaluated and the therapeutic efficacy of ADC measurement assessed in comparison with conventional MRI.

METHODS

One-hundred sixty-eight patients with tumors of the brain underwent STI in our hospital between September 2002 and April 2004. In 39 patients, DWI before and after STI was prospectively performed to evaluate change in ADC of the tumor between October 2003 and April 2004. Nineteen patients with tumors more than 10-mm in size were included in the present study, because other 20 patients had tumors less than 10-mm in size or tumors near the base of the skull. In these 19 patients, informed consent for MRI before and after STI was obtained. The tumors consisted of metastatic tumors (n = 10), glioblastomas (n = 3), meningiomas (n = 2), malignant lymphoma (n = 1), schwannoma (n = 1), chordoma (n = 1), and primitive neuroectodermal tumor (n = 1). The primary tumors of the metastatic tumors were carcinomas of the lung (n = 7), breast (n = 2), and uterus (n = 1). Nine patients with other than metastatic tumors were diagnosed by biopsy or partial removal of the tumor. In these 9 patients, MRI before STI was performed more than 2 weeks after surgery. MRI was performed using a 1.5-T unit (GE Medical Systems, Milwaukee, WI), and axial spin-echo (SE) T1-weighted images (TIWI) (380–680/9–14/4 [repetition time millisecond per echo time millisecond per number of excitations], 4-mm slice thickness, 2-mm interslice gap), axial fast SE T2-weighted images (T2WI) (3600–4500/96–105[effective]/2, echo train length; 10–16, 4-mm slice thickness, 2-mm interslice gap), fast SE fluid-attenuated inversion-recovery (FLAIR) (1002/148–162/1, inversion time (TI); 2200, echo train length; 8, 4-mm slice thickness, 2-mm interslice gap), contrast-enhanced T1WI (T1WI(+)) after intravenous administration of 0.2 mmol/kg of body weight gadopentitate dimeglumine (Magnevist; Nihon Schering, Osaka, Japan), and DWI were acquired within 1 week before STI and 2–4 weeks after STI. DWI was performed using

From the *Department of Radiology; †Department of Neurosurgery, Akita University School of Medicine; and ‡Department of Radiology, Akita University Hospital.
Received for publication November 23, 2005; accepted February 1, 2006.
Reprints: Noriaki Tomura, MD, Department of Radiology, Akita University School of Medicine, 1-1-1, Hondo, Akita city, Akita, 010-8543, Japan (e-mail: tomura@med.akita-u.ac.jp).

a single-shot SE-planar imaging sequence by applying diffusion gradients in 3 orthogonal directions for each section, with 2 diffusion weightings (b = 0 s/mm^2 and 1000 s/mm^2). Isotropic DWI was acquired by averaging 3 orthogonal images. The imaging parameters for DWI were as follows: TR/TE/NEX; 10,000/100/1, 4-mm section thickness, 2-mm intersection gaps, 128 × 128 matrix, 220-mm field of view. All DWI images were transferred to a workstation Dr. View/PRO Release 5.0 (Asahi Kasei Corporation Systems, Co., Ltd., Tokyo), at which ADC maps were calculated. Regions of interest (ROIs) were drawn manually on the tumor, peritumoral regions, and their corresponding areas in the contralateral cerebral hemisphere using the axial T1WI(+). The ROI ranged from 36 to 87 mm^2. ROIs in the tumor included the area with maximal degree of contrast enhancement on T1WI(+). All tumors enhanced after contrast administration. In tumors with different site of contrast enhancement, such as glioblastomas, ROIs were set in these different sites. Number of ROIs in the tumor ranged from 1 to 3. ROIs in the peritumoral region were set around the contrast-enhanced tumor on T1WI(+). Number of ROIs in the peritumoral region ranged from 2 to 5. The mean ADC in the tumor and peritumoral region was measured. The mean ADC was normalized (nADC) by dividing ADC values of the corresponding areas in the contralateral cerebral hemisphere. Follow-up MRI, including T1WI, T2WI, FLAIR, and T1WI(+), was performed to evaluate the changes in tumor size. The maximum diameter of the tumor was measured on the postcontrast T1WI before STI, 2–4 weeks after STI, and 8–12 weeks after STI.

STI was administered using a stereotactic headring frame (BrainLAB AG, Munich, Germany), with a dedicated linear accelerator (Varian Clinac 600C). STI was delivered to the margin of the lesion with a range of 10.75–45.36 Gray (Gy) and the maximum doses ranged from 21.6 to 57.12 Gy. Target volume ranged from 4.02 to 30.85 cm^3, whereas the number of fractions in STI ranged from 1 to 5.

The nADC in the tumor and peritumoral region before STI was compared with that after STI, and the change in the nADC of the tumor was compared with the change in tumor size measured on T1WI(+). The time independence (within 1 week before STI, 2–4 weeks after STI) of the nADC of the tumor and peritumoral region was justified using a paired Student *t* test. Treatment response of the tumor was evaluated by MRI at 2–4 weeks and 8–12 weeks after STI. The nADC of the tumor was compared between the responder and nonresponder groups evaluated by MRI at 2–4 weeks and 8–12 weeks after STI. An increase or no change in tumor size in postcontrast T1WI compared with tumor size before STI was interpreted as a nonresponse to treatment. The difference in the nADC of the tumor 2–4 weeks after STI between the responder and nonresponder groups was justified using Student *t* test. For statistical tests, a *P* value less than 0.05 was considered to indicate statistical significance.

RESULTS

Change of tumor size and nADC before and after STI was indicated in Table 1. The nADC of the tumors was significantly greater at 2–4 weeks after STI (mean ± SD = 1.91 ± 1.67) than before STI (1.40 ± 0.99) (Fig. 1). Especially, 3 tumors, that is 1 primitive neuroectodermal tumor (PNET) and 2 metastatic tumors, showed a dramatic difference in nADC before and after STI. The nADC of the peritumoral region at 2–4 weeks after STI (1.29 ± 0.69) did not differ significantly from that before STI (1.59 ± 1.92). No significant difference in the nADC at 2–4 weeks after STI was observed between the responder (1.95 ± 1.82) and nonresponder (1.87 ± 1.60) groups evaluated by MRI at 2–4 weeks after STI (Fig. 2). However, there was a significant difference in the nADC at 2–4 weeks after STI between the responder (2.52 ± 1.93) and nonresponder (1.00 ± 0.36) groups when evaluated by MRI at 8–12 weeks after STI (Fig. 3). All 3 tumors (1 PNET and 2 metastatic tumors) with dramatically increased nADC after STI showed a remarkable response for STI. In pathologically benign tumors, such as meningiomas, schwannomas, and chordomas, the value of nADC little changed after STI; however, there was not a significant difference in change of nADC between pathologically benign and malignant tumors. Figure 4 shows a representative case, with the metastatic tumor originating from carcinoma of the lung. The patient underwent STI with 26.2 Gy to the periphery of the tumor. The nADC before STI was 1.29 in the tumor and 2.03 in the peritumoral region, and changed to 1.86 in the tumor and 1.28 in the peritumoral region after STI, although the tumor did not significantly

TABLE 1. Change of Tumor Size and nADC Before and After STI

Case No.	Pathology	Tumor Size before STI (mm)	Tumor Size 2–4 weeks after STI (mm)	Tumor Size 8–12 weeks after STI (mm)	Tumor nADC Before STI	Tumor nADC 2–4 weeks after STI
1	Metastasis	23	16	30	0.66	1.28
	Metastasis	23	18	18	0.51	2.57
2	Metastasis	23	23	20	1.61	1.7
3	Metastasis	26	23	12	1.29	1.86
4	Metastasis	16	14	11	4	5.55
5	Metastasis	18	15	15	2.09	1.71
6	Metastasis	15	16	23	1.23	1.41
7	GBM	30	27	32	0.46	0.62
8	GBM	16	14	32	0.32	0.33
9	GBM	20	20	12	1.23	1.39
10	PNET	12	13	6	2.94	7.08
11	ML	14	10	0	0.2	0.37
12	Meningioma	28	32	36	0.88	1.1
13	Meningioma	21	25	22	1.1	1.17
14	Chordoma	22	22	30	0.78	0.95
15	Schwannoma	22	19	18	3.2	3.3
16	Metastasis	35	40	21	1.59	1.8
17	Metastasis	13	14	11	1.53	1.61
18	Metastasis	38	38	34	1.25	1.27
19	Metastasis	21	17	22	1.2	1.13

nADC indicates ADC in the tumor divided by ADC in the corresponding area in the contralateral cerebral hemisphere; GBM, glioblastoma; PNET, primitive neuroectodermal tumor; ML, malignant lymphoma.

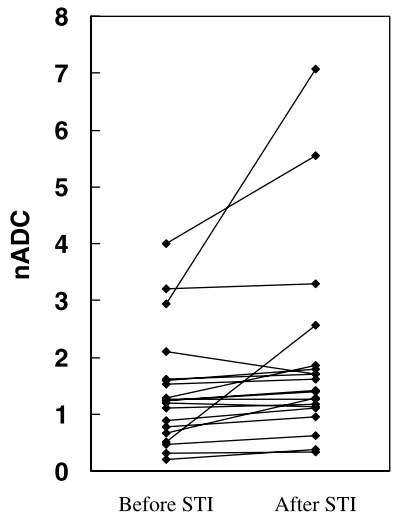

FIGURE 1. The nADC of a tumor 2–4 weeks after STI (mean ± SD = 1.91 ± 1.67) was significantly ($P < 0.05$) higher than that before STI (1.40 ± 0.99). nADC indicates ratio of the ADC for the tumor or peritumoral region to that of the normal contralateral region.

change in size. The tumor had significantly decreased in size at 12 weeks after STI, as determined by T1WI(+).

DISCUSSION

The changes in the ADC induced by STI were determined, as was whether treatment-induced changes in tumors can alter the tumor ADC before a change in tumor size is noted. An increase in the nADC of tumors after STI was found. The ADC of a tumor is thought to reflect the degree of cellularity and nuclear-to-cytoplasmic (N/C) ratio.[11] Chemotherapy and radiotherapy decrease cellularity and increase the ratio of the extracellular volume to intracellular volume. The present

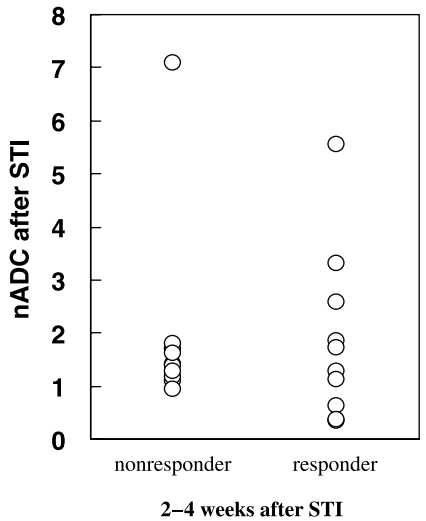

FIGURE 2. The nADC of tumors 2–4 weeks after STI in the responder (1.95 ± 1.82) and nonresponder (1.87 ± 1.60) groups, as evaluated by MRI at 2–4 weeks after STI. No significant difference in nADC was observed.

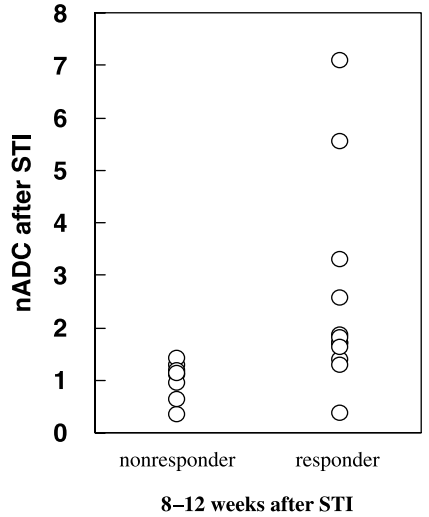

FIGURE 3. The nADC of tumors 2–4 weeks after STI in the responder (2.52 ± 1.93) and nonresponder (1.00 ± 0.36) groups, as evaluated by MRI at 8–12 weeks after STI. A significant difference ($P < 0.05$) in nADC was observed.

results indicate that a change in the nADC precedes a change in tumor size and DWI is a sensitive tool with which to monitor tumor response to treatment. All the tumors with a value of nADC greater than 1.41 showed a response to STI (Fig. 3).

Recent observations in several animal studies have found an increased ADC after radiation, gamma knife irradiation, chemotherapy, or gene therapy.[18–22] Their histological examinations confirmed that treatment caused a loss of cells, presence of necrotic damage, or cytoplasmic shrinkage. Most of these animal studies performed MRI several days after treatment. Zhao et al[18] studied ADC change after cyclophosphamide treatment in implanted murine tumors and confirmed an increased ADC of the tumor several days after treatment with no change in tumor volume. Their results with animal tumors indicate that ADC measurement is likely a good response indicator and were consistent with our results in human tumors of the brain. In human tumors, Theilmann et al[16] measured the ADC of liver metastases before and after chemotherapy and found that the ADC of the tumor increased 4 or 11 days after treatment in the responder group of patients. Their data also suggested that measurement of the ADC of a tumor can predict the response of liver metastases to chemotherapy. On the other hand, other reports have documented a decreased ADC after tumor treatment. Hein et al[15] reported a decrease in the ADC in human rectal carcinomas in the second, third, and fourth week of chemoradiation. Cytotoxic edema and fibrosis were thought to have induced this decrease in the ADC. In their study, the ADC was measured during the course of chemoradiation. As in the acute phase of cerebral infarct, the phenomenon of cytotoxic edema can be observed during or immediately after treatment. In the present study, ADC measurement was performed 2–4 weeks after treatment. Minamikawa et al[20] also observed the increase in ADC of brain tumors and normal white matter 1–27 days after glucocorticoid treatment. However, their results seem to reflect glucocorticoid effects, which restrict movement of water molecules and

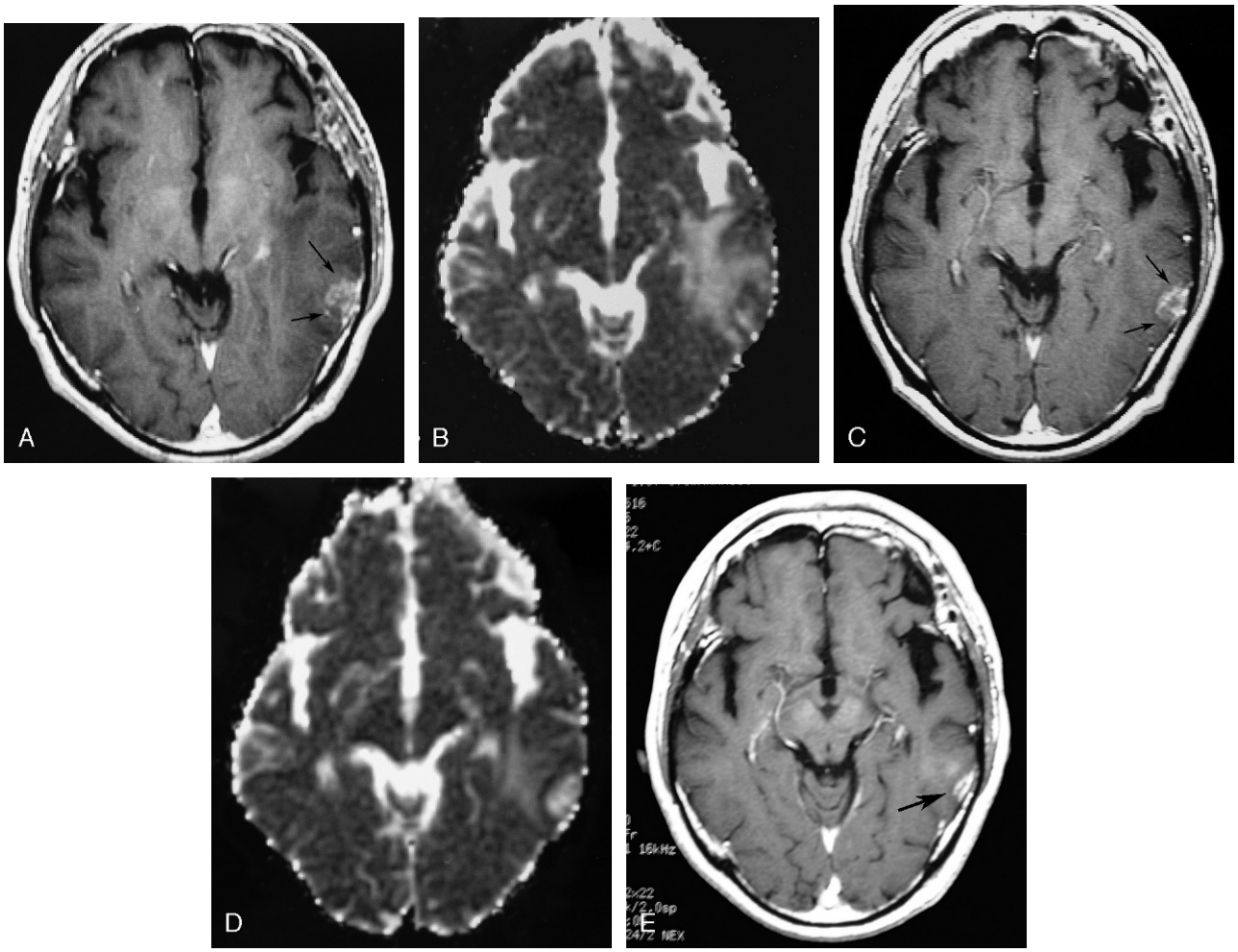

FIGURE 4. A case with metastatic tumor (A) (arrows) originating from carcinoma of the lung. The patient underwent STI with 26.2 Gy to the periphery of the tumor. The nADC before STI (B) was 1.29 in the tumor and 2.03 in the peritumoral region, and 1.86 in the tumor and 1.28 in the peritumoral region after STI (D), although the tumor had not significantly changed in size (C) (arrows). The tumor significantly decreased in size (E) (arrow), as seen in T1WI(+) at 12 weeks after STI. A, T1WI(+) before STI; B, DWI before STI; C, T1WI(+) 2 weeks after STI; D, DWI 2 weeks after STI; E, T1WI(+) 12 weeks after STI.

albumin even through the normal blood–brain barrier. In the present study, 8 patients received steroids at the times of MR studies before and after STI. It seemed to reflect little on the results, because steroids administration was performed at the time of both MR studies before and after STI.

Transient enlargement of a tumor has sometimes been seen after STI treatment,[23] in particular, in the histology of benign tumors such as schwannomas and meningiomas. In the present study, 3 of 4 tumors of histologically benign nature showed a slight increase in size at 2–4 weeks after STI.

Radiological evaluation of STI has been previously performed using FDG-PET and Tl-SPECT.[5–10] Evaluation of the response to treatment by ADC measurement has several advantages over these other modalities. It is noninvasive without radiation exposure. FDG-PET has high sensitivity and specificity in differentiating between radiation necrosis and tumor progression in brain tumors.[24,25] However, PET scanners and cyclotrons are still not available widespread. Tl-SPECT has also high sensitivity for differentiating between radiation necrosis and tumor progression;[26] however its spatial resolution is low. MR spectroscopy (MRS) can detect altered levels of biochemical tissue compounds and has also been used to differentiate radiation necrosis from tumor recurrence and to evaluate treatment response.[27,28] The ratio of choline to creatine was found to be a more sensitive tool in evaluating the response to stereotactic radiosurgery than Tl-SPECT or conventional MRI. For instance, a reduction in the choline/creatine ratio was noted in metastatic brain tumors the day after gamma knife radiosurgery.[27,29] However, to our knowledge, a comparison of ADC measurement to MRS has not been performed yet, as far as monitoring response to treatment is concerned. As ADC measurement of a tumor is almost the same as MRS, the value depends on the location of the measurement in cases with inhomogeneous tumor. In the present study, the ADC was measured only in the solid components with contrast enhancement on MRI.

The present study has some limitations. This study was not performed using consecutive patients, and the number of

tumors examined was small. Further studies with a larger sample size are required. If more patients with metastases were studied, result limited in metastases may be better. Furthermore, the subjects had several kinds of tumors such as gliomas, metastases, and benign tumors. In future, benign tumors, such as meningiomas, schwannomas, and chordomas, can be examined separately from malignant tumors. Another limitation was that the manual drawing of the ROIs may have been subjective. However, manual drawing was necessary due to the inhomogeneous components of the gliomas. ROIs were set only on the solid components. In the glioblastomas, the ROIs in the peritumoral region may have included tumor tissue to some degree. Similarly, in the other cases with different kinds of tumors, the ROIs in the peritumoral region may have included tumor tissue due to spatial distortion of DWI as a result of the single-shot echo-planar sequence. Multishot echo-planar sequence will reduce this distortion.[30]

CONCLUSIONS

Changes in the nADC measured by DWI can predict response to STI. These changes are preceded by more than 4-week changes in tumor size as evaluated by conventional MRI, enabling the efficacy of STI to be determined earlier. Thus, when no increase in the nADC is evident after STI, treatment strategies can be changed without needing to wait for a change in tumor size.

REFERENCES

1. Chidel MA, Suh JH, Reddy CA, et al. Application of recursive partitioning analysis and evaluation of the use of whole brain radiation among patients treated with stereotactic radiosurgery for newly diagnosed brain metastases. *Int J Radiat Oncol Biol Phys*. 2000;47:993–999.
2. Plathow C, Schulz-Ertner D, Thilman C, et al. Fractionated stereotactic radiotherapy in low-grade astrocytomas: long-term outcome and prognostic factors. *Int J Radiat Oncol Biol Phys*. 2003;57:996–1003.
3. Milker-Zabel S, Zabel A, Schulz-Ertner D, et al. Fractionated stereotactic radiotherapy in patients with benign or atypical intracranial meningiomas: long-term experience and prognostic factors. *Int J Radiat Oncol Biol Phys*. 2005;61:809–816.
4. Muacevic A, Jess-Hempen A, Tonn JC, et al. Results of outpatient gamma knife radiosurgery for primary therapy of acoustic neuromas. *Acta Neurochir Suppl*. 2004;91:75–78.
5. Ericson K, Kihlstrom L, Mogard J, et al. Positron emission tomography using ^{18}F-fluorodeoxyglucose in patients with stereotactically irradiated brain metastases. *Stereotact Funct Neurosurg*. 1996;66(suppl. 1): 214–224.
6. Maruyama I, Sadato N, Waki A, et al. Hyperacute changes in glucose metabolism of brain tumors after stereotactic radiosurgery: a PET study. *J Nucl Med*. 1999;40:1085–1090.
7. Yamamoto T, Nishizawa S, Maruyama I, et al. Acute effects of stereotactic radiosurgery on the kinetics of glucose metabolism in metastatic brain tumors: FDG PET study. *Ann Nucl Med*. 2001; 15:103–109.
8. Kline JL, Noto RB, Glantz M. Single-photon emission CT in the evaluation of recurrent brain tumor in patients treated with gamma knife radiosurgery or conventional radiation therapy. *AJNR Am J Neuroradiol*. 1996;17:1681–1686.
9. Seo Y, Fukuoka S, Nakagawara J, et al. Early effects of gamma knife radiosurgery on brain metastases: assessment by ^{201}TlCl SPECT and ^{99m}Tc-DTPA-human serum albumin SPECT. *Neurol Med Chir (Tokyo)*. 1997;37:25–31.
10. Kimura T, Sako K, Tanaka K, et al. Evaluation of the response of metastatic brain tumors to stereotactic radiosurgery by proton magnetic resonance spectroscopy, ^{201}TlCl single-photon emission computerized tomography, and gadolinium-enhanced magnetic resonance imaging. *J Neurosurg*. 2004;100:835–841.
11. Guo AC, Cummings TJ, Dash RC, et al. Lymphomas and high-grade astrocytomas: comparison of water diffusibility and histologic characteristics. *Radiology*. 2002;224:177–183.
12. Stadnik TW, Chaskis C, Michotte A, et al. Diffusion-weighted MR imaging of intracerebral masses: comparison with conventional MR imaging and histologic findings. *AJNR Am J Neuroradiol*. 2001; 22:969–976.
13. Yamasaki F, Kurisu K, Satoh K, et al. Apparent diffusion coefficient of human brain tumors at MR imaging. *Radiology*. 2005;235:985–991.
14. Valonen PK, Lehtimaki KK, Vaisanen TH, et al. Water diffusion in a rat gliomas during ganciclovir-thymidine kinase gene therapy-induced programmed cell death in vivo: correlation with cell density. *J Magn Reson*. 2004;19:389–396.
15. Hein PA, Kremser C, Judmaier W, et al. Diffusion-weighted magnetic resonance imaging for monitoring diffusion changes in rectal carcinoma during combined, preoperative chemoradiation: preliminary results of a prospective study. *Eur J Radiol*. 2003;45:214–222.
16. Theilmann RJ, borders R, Trouard TP, et al. Changes in water mobility measured by diffusion MRI predict response of metastatic breast cancer to chemotherapy. *Neoplasia*. 2004;6:831–837.
17. Liapi E, Kamel IR, Bluemke DA, et al. Assessment of response of uterine fibroids and myometrium to embolization using diffusion-weighted echoplanar MR imaging. *J Comput Assist Tomogr*. 2005;29:83–86.
18. Zhao M, Pipe JG, Bonnett J, et al. Early detection of treatment response by diffusion-weighted ^{1}H-NMR spectroscopy in a murine tumour in vivo. *Br J Cancer*. 1996;73:61–64.
19. Chinnaiyan AM, Prasad U, Shankar S, et al. Combined effect of tumor necrosis factor-related apoptosis-inducing ligand and ionizing radiation in breast cancer therapy. *Proc Natl Acad Sci*. 2000;97:1754–1759.
20. Minamikawa S, Kono K, Nakayama K, et al. Glucocorticoid treatment of brain tumor patients: changes of apparent diffusion coefficient values measured by MR diffusion imaging. *Neuroradiology*. 2004;46:805–811.
21. Herynek V, Burian M, Jirak D, et al. Metabolite and diffusion in the rat brain after Leksell Gamma Knife irradiation. *Magn Reson Med*. 2004;52:397–402.
22. Thoeny HC, Keyzer FD, Chen F, et al. Diffusion-weighted MR imaging in monitoring the effect of a vascular targeting agent on rhabdomyosarcoma in rats. *Radiology*. 2005;234:756–764.
23. Pan DHC, Guo WY, Chung WY, et al. Early effects of gamma knife surgery on malignant and benign intracranial tumors. *Stereotact Funct Neurosurg*. 1995;64(suppl. 1):19–31.
24. Mogard J, Kihlstrom L, Ericson K, et al. Recurrent tumor vs radiation effects after gamma knife radiosurgery of intracerebral metastases: diagnosis with PET-FDG. *J Comput Assist Tomogr*. 1994;18:177–181.
25. Ericson K, Kihlstrom L, Mogard J, et al. Positron emission tomography using ^{18}F-fluorodeoxyglucose in patients with stereotactically irradiated brain metastases. *Stereotact Funct Neurosurg*. 1996;66(suppl. 1): 214–224.
26. Schwartz RB, Carvalho PA, Alexander E III, et al. Radiation necrosis vs high-grade recurrent glioma: differentiation by using dual-isotope SPECT with 201Tl and 99mTc-HMPAO. *AJNR Am J Neuroradiol*. 1991;12:1187–1192.
27. Chernov MF, Hayashi M, Izawa M, et al. Early metabolic changes in metastatic brain tumors after Gamma knife radiosurgery: ^{1}H-MRS study. *Brain Tumor Pathol*. 2004;21:63–67.
28. Rock JP, Scarpace L, Hearshen D, et al. Associations among magnetic resonance spectroscopy, apparent diffusion coefficients, and image-guided histopathology with special attention to radiation necrosis. *Neurosurgery*. 2004;54:1117–1119.
29. Tarnawski R, Sokol M, Pieniazek P, et al. 1H-MRS in vivo predicts the early treatment outcome of postoperative radiotherapy for malignant gliomas. *Int J Radiat Oncol Biol Phys*. 2002;52:1271–1276.
30. Tomura N, Kato K, Takahashi S, et al. Multi-shot echo-planar fluid-attenuated inversion-recovery imaging with fast SE fluid-attenuated inversion-recovery and T2-weighted imaging in depiction of white matter lesion. *J Comput Assist Tomogr*. 2002;26:810–814.